

Harry Tauber
Vice President
Engineering and Construction

Detroit
Edison

2000 Second Avenue
Detroit, Michigan 48226
(313) 237-5000

September 9, 1982
EF2 - 59,222

Mr. B. J. Youngblood, Chief
Licensing Branch No. 1
Division of Licensing
U. S. Nuclear Regulatory Commission
Washington, D. C. 20555

Dear Mr. Youngblood:

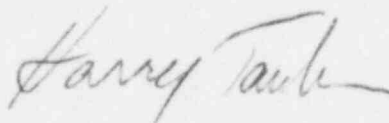
Reference: Enrico Fermi Atomic Power Plant, Unit 2
NRC Docket No. 50-341

Subject: Mark I Containment
Request For Additional Information

Attached please find our response to your July 19, 1982 request for additional information on the Fermi 2 Plant Unique Analysis Report (PUAR). Due to the time constraint, the response is submitted in the question/response format. After you have reviewed and accepted our response, we will incorporate the attachment into the PUAR, revising PUAR pages if applicable.

If you have any questions regarding the above, please contact Mr. Larry E. Schuerman, (313) 649-7562.

Sincerely,



Attachment

cc: Mr. L. L. Kintner
Mr. J. Ranlet (Brookhaven National Laboratories)
Mr. W. Seagraves (Franklin Research Institute)

8209140298 820909
PDR ADOCK 05000341
A PDR

A025

Question 10.1

With regard to suppression chamber analysis, provide justification for not analyzing a 180° beam segment including the torus, columns, and seismic restraints as required by the criteria for considering the effect of seismic and other lateral loads. Also, discuss the implications of this approach with regard to stresses in the suppression chamber in the region surrounding the support columns.

Response to Question 10.1

The approach used in the Fermi PUAR to evaluate suppression chamber lateral loads results in total lateral loads which envelop those which would be obtained by a 180° beam model. As discussed in PUAR Section 4-2.4.2, maximum accelerations and dynamic load factors are used to develop bounding values of lateral loads for seismic loads and for asymmetric torus shell loads due to SRV discharge and pre-chug, irrespective of the suppression chamber frequency. Specifically, the maximum OBE spectral acceleration of 0.23g is used for seismic loads, the maximum dynamic load factor of 2.60 is used for SRV discharge loads, and the maximum dynamic load factor of 13.9 is used for pre-chug loads each of which occurs at a different frequency. The resulting lateral loads for the seismic, SRV discharge, and pre-chug loadings are added absolutely to obtain a bounding value of the total suppression chamber lateral load, which is conservatively assumed to be transferred by two of the four seismic restraints.

The total lateral load which would be produced by a 180° beam model would be less since the response to each loading would primarily be determined at the dominant lateral frequency of the suppression chamber.

Lateral loads result in a shear effect and an overturning moment effect on the suppression chamber. The horizontal shear effect is the more significant component and is resisted by the seismic restraints shown in Figure 2-2.1-10. The overturning moment effect results in vertical loads which are resisted at each mitered joint by the suppression chamber columns and mitered joint saddles shown in Figure 2-2.1-4. The vertical loads on any one column/saddle assembly are small compared with those caused by the major torus shell loadings which primarily act in the vertical direction, the results of which are shown in Table 2-2.5-4. The corresponding stresses in the suppression chamber shell adjacent to the column/saddle assembly due to the overturning moment would also be small.

Question 10.2

With regard to the assumption that only 20% of the total mass of water in the suppression chamber contributes to lateral seismic loads, provide justification to indicate the applicability of the tests cited in the PUA report to support this assumption.

Response to Question 10.2

For a suppression chamber partially filled with water subjected to a horizontal seismic excitation, a portion of the total water mass acts as a rigidly attached mass while the remaining water mass acts in sloshing modes. The effective weight of water which acts as a rigidly attached mass was determined from 1/30 scale generic tests performed as part of the Mark I program effort. The seismic slosh test facility is identical and the test procedures used to determine the effective water weight are similar to the tests described in General Electric Report NEDC-23702-P, "Mark I Containment Program Seismic Slosh Evaluation", March 1978.

The 1/30 scale model test facility is based on a prototypical Mark I suppression chamber whose geometric characteristics are very close to those of Fermi 2. Tests were performed with three different support stiffnesses (rigid, medium, and flexible), which covered the range of stiffnesses and frequencies for all Mark I plants, including Fermi 2.

The analytical model developed for use in the referenced study predicts that 20% of the total mass of water acts as a rigidly attached mass with the suppression chamber. This

prediction was verified with the 1/30 scale model by comparing the measured frequencies of the test facility with those obtained from the analytical model. This was done by first adjusting the emptied test facility support stiffness to that necessary to obtain the frequency of the empty suppression chamber predicted by the analytical model. The test facility was subsequently filled with water to a height below the equator, and a series of tests were performed to determine the frequency. The resulting frequencies compared favorably with those obtained using the analytical model with the same assumed water height. The test results therefore confirm the analytical results which showed that 20% of the total water mass acts as a rigidly attached mass. These results are considered applicable for use in evaluating the Fermi 2 suppression chamber response to seismic loadings.

The evaluation of the Fermi 2 suppression chamber for horizontal seismic loads is discussed in Section 2-2.4.2 of the PUAR. The seismic lateral load is conservatively calculated assuming that 20% of the total water mass acts at the maximum spectral acceleration of 0.23g. The remaining 80% of water is assumed to act at the maximum accelerations in the range of sloshing frequencies. The methodology accounts for 100% of the water and results in a bounding value for the suppression chamber lateral load due to seismic loads.

Question 10.3a

Provide detailed calculations to indicate how the modal correction factors given in Sections 1-4.2.3 and 2-2.4.1 of the PUA report are obtained.

Response to Question 10.3a

Modal correction factors used in calculating the response due to SRV torus shell loads are obtained by dividing the response of an initial value or free vibration problem by that of a transient forced vibration response problem. The physical representations for the analogs used in developing these correction factors are shown in Figure 10.3-1. Two representations of source pressure in a rigid tank are shown. The transient response problem consists of a rigid torus with a pressure source, P_B , which is prescribed as a decaying cosine function. The initial value problem consists of a similar torus which contains a spring and disk mechanism for providing an impulse to the surrounding pool water.

The analogs, described in terms of masses and springs, are shown in Figure 10.3-2 for the transient response or forced vibration problem and the initial value or free vibration problem. The torus system is described in terms of a generalized stiffness, k_s , and a generalized mass, m_s .

The forced vibration analog is subjected to an applied loading, described as

$$P_B(t) = P_B e^{-\lambda t} \cos \omega_B t$$

where,

- P_B = bubble force at time equal to zero
- λ = attenuation constant
- ω_B = frequency of the SRV bubble
- t = time

The free vibration analog incorporates an additional mass and spring, representing the bubble system, which is utilized to establish a frequency of the bubble oscillation. The apparent or effective mass of the bubble is defined as m_B . The numerical value of an apparent bubble mass is estimated by averaging the hydrodynamic mass for the case of an oscillating sphere in a still fluid and a fixed sphere in an oscillating fluid. The bubble stiffness is computed by multiplying the bubble mass by the bubble frequency squared.

Four spherical bubbles are assumed for the T-quencher discharge device. Single bubble stiffnesses are additive since the bubbles are assumed to act in phase (i.e., parallel springs).

The initial conditions for the free vibration analog are prescribed by compressing the spring, k_B , a distance, Δl , such that at time equal to zero the force in the spring is equal to P_B . Therefore, at time equal to zero, both the forced vibration and free vibration analog have the same applied load magnitude.

Damping for the torus system can be described in terms of load attenuation and structural damping. Based upon test observations, it is assumed that the structural response will be decayed in the same manner as the prescribed pressure. Accordingly, a decaying exponential function of the form $e^{-\lambda t}$ is used to represent load attenuation and structural damping in the solution of the forced and free vibration system, respectively.

The equations of motion for the free vibration analog described in Figure 10.3-2 are obtained from free body diagrams for the structure mass and bubble mass as

$$m_s \ddot{X}_s - (k_s + k_B) X_s + k_B X_B = 0$$

$$m_B \ddot{X}_B - k_B X_B + k_B X_s = 0$$

where,

X_s	=	structure mass displacement
\ddot{X}_s	=	structure mass acceleration
X_B	=	bubble mass displacement
\ddot{X}_B	=	bubble mass acceleration

The solution to these equations expressed in terms of the structure response, X_s , is given as the following function,

$$X_s = \frac{P_B}{k_s} e^{-\lambda t} f_1\left(\frac{\omega_B}{\omega_s}, \frac{k_B}{k_s}, \frac{m_B}{m_s}\right)$$

where,

ω_B = bubble frequency

ω_s = structure frequency

The other variables have been previously defined.

A family of curves which represents dynamic load factors as a function of frequency (ω_B/ω_s) is generated by assuming either (k_B/m_s) or (m_B/m_s) as constant. Based upon estimates of the significant modal characteristics of the torus and the oscillating bubble, a range of values for (k_B/m_s) and (m_B/m_s) is established. The range of (k_B/m_s) values is estimated to be about 160 to 1600. The range of (m_B/m_s) values is estimated to be 0.03 to 0.3.

Figure 10.3-3 contains a comparison of DLF's for the cases with (k_B/m_s) equal to 160 and 1600, assuming a structural frequency of 20 hz. The maximum DLF for the case with (k_B/m_s) equal to 160 is 2.8, whereas for (k_B/m_s) equal to 1600, the maximum DLF is 2.0. It was determined that the DLF's for the case with (k_B/m_s) equal to a constant are about 20 to 60 percent larger than the DLF's for the case with (m_B/m_s) equal to a constant.

The equation of motion for the forced vibration analog described in Figure 10.3-2 is obtained from the free body diagram for the structure mass as

$$m_s X_s - k_s X_s = P_B e^{-\lambda t} \cos \omega_B t$$

The solution to this equation is given in the following function:

$$X_s = \frac{P_B}{k_s} e^{-\lambda t} f_2(\omega_B, \omega_s, \lambda)$$

Figure 10.3-4 contains DLF's plotted as a function of (ω_B/ω_s) . A family of DLF curves is included for structure frequencies of 11, 14, 20 hz. The DLF's for the resonant condition range from 5.4 to 9.9 for structural frequencies between 11 and 20 hz. The forced vibration DLF's are approximately 3 to 5 times the free vibration DLF's.

Correction factors are obtained by dividing the free vibration response to the system by the response of the forced vibration system. The sensitivity of the correction factor to the variables $(k_b/m_s, m_b/m_s, \lambda)$ is evaluated in order to determine a valid set of correction factor curves to be used in design.

Based upon the above evaluation, it was determined that the lower range of (k_b/m_s) should be used for determining conservative design basis modal correction factors. An

attenuation factor of 6 is selected, since use of this factor results in correction factors which bound the response at resonance conditions for all structural frequencies.

A typical correction factor curve is shown in Figure 10.3-5 for a structural frequency of 20 hz. For the plant unique analysis, a set of enveloping correction factors is generated for different modal frequencies of interest as shown in PUAR Figure 2-2.4-5.

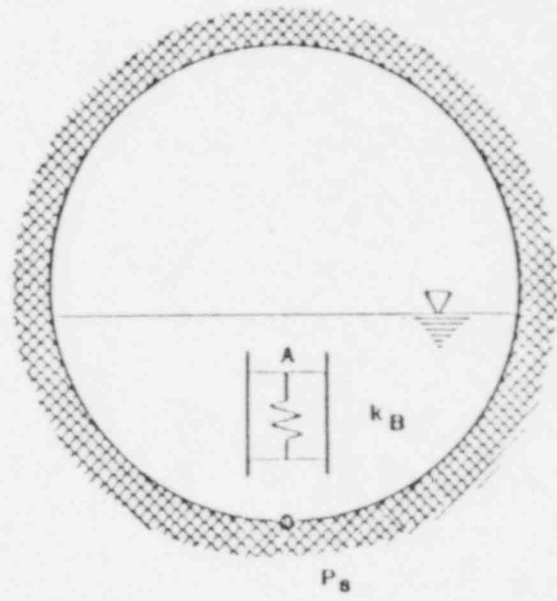
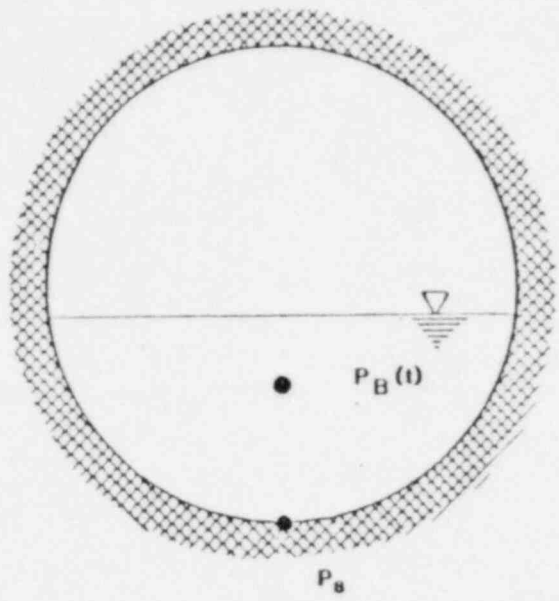
Table 10.3-1 contains a comparison of analytical results obtained using modal correction factors and measured results for Monticello. The results shown are obtained by dividing analytical results by test results for key response parameters. The comparisons show that modal correction factors provide a conservative basis for calibrating the analytical model used to evaluate the response of the Fermi-2 suppression chamber for SRV torus shell loads. The modal correction factors are developed at test conditions and applied at design conditions in accordance with NUREG-0661.

Location	Component	Test Condition	
		Cold Pop	Hot Pop
	a) Stress Intensity		
78° From Inside Equator Midbay	Shell Membrane	1.2	1.3
78° From Outside Equator Midbay	Shell Membrane	1.4	2.3
	b) Column Reaction		
Inside Support Column	Upload	3.7	3.0
Inside Support Column	Download	2.8	2.0
Outside Support Column	Upload	4.4	3.5
Outside Support Column	Download	2.7	2.8

Table 10.3-1 - Corrected Transient Response Analysis
Normalized by Test Response

$$P_B(t) = P_B e^{-\lambda t} \cos \omega_B t$$

$$\text{AT TIME ZERO: } P_B = \frac{k_B \Delta l}{A}$$



a) TRANSIENT DEFINITION

b) INITIAL VALUE DEFINITION

Figure 10.3-1 - SRV Load Definition

DET-15-020
Revision 0

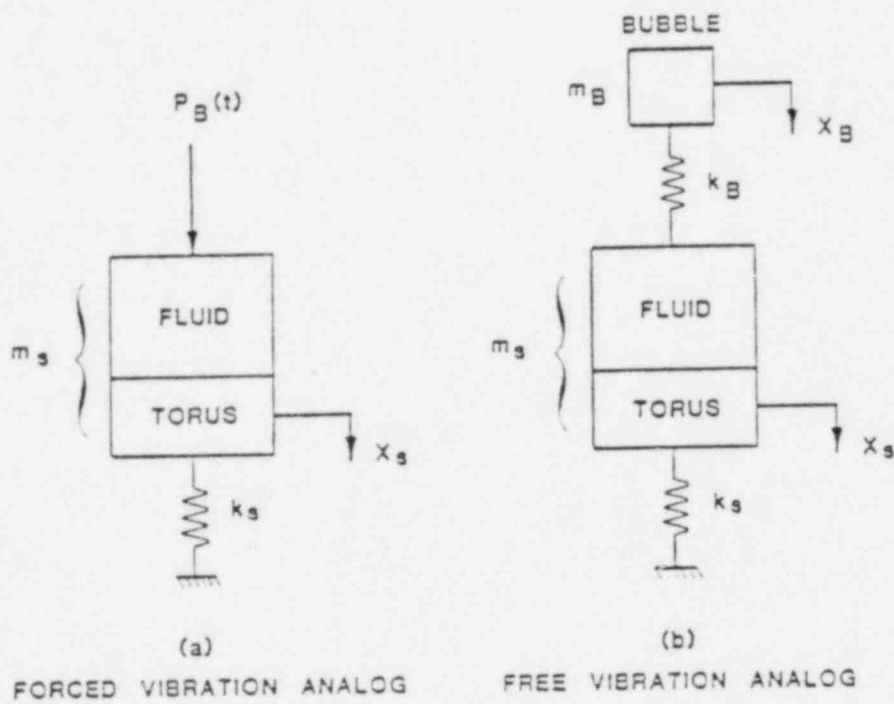


Figure 10.3-2 - Structural Response Analogs

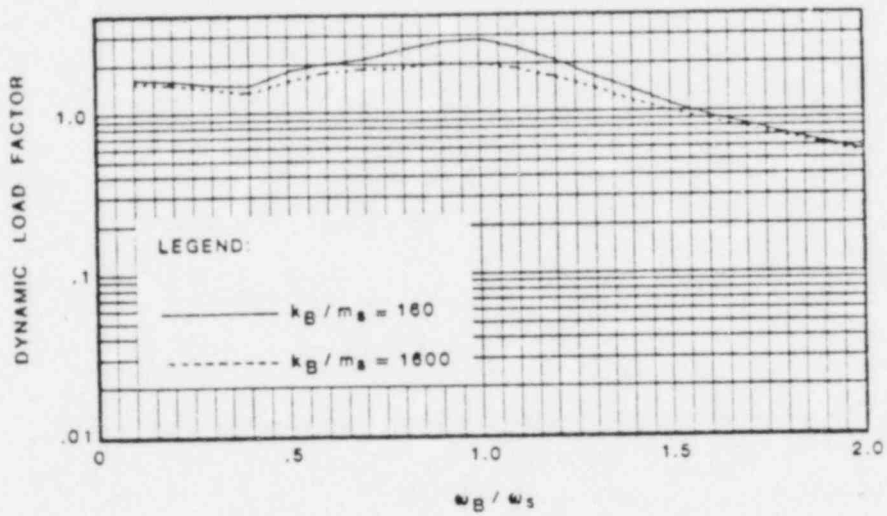


Figure 10.3-3 - Free Vibration Analog Dynamic Load Factors
For (k_B/m_s) Constant

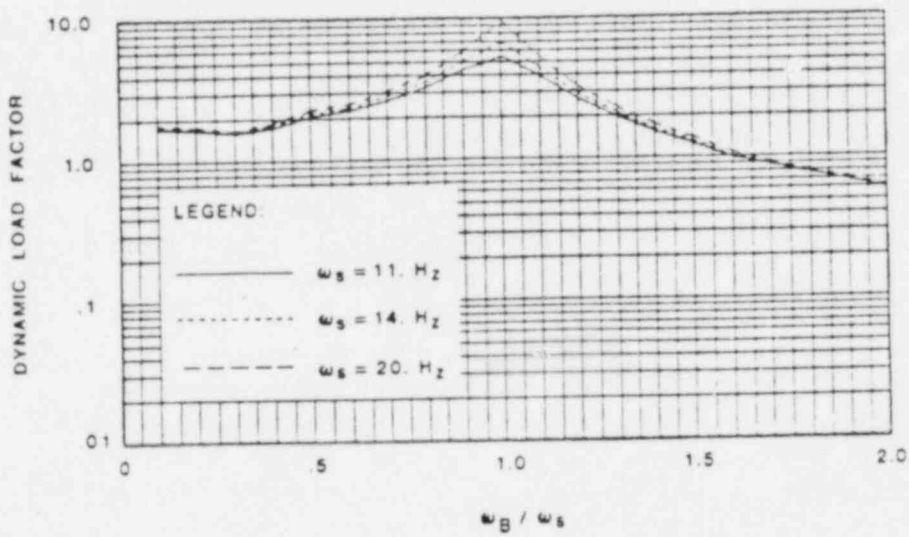


Figure 10.3-4 - Forced Vibration Analog Dynamic Load Factors

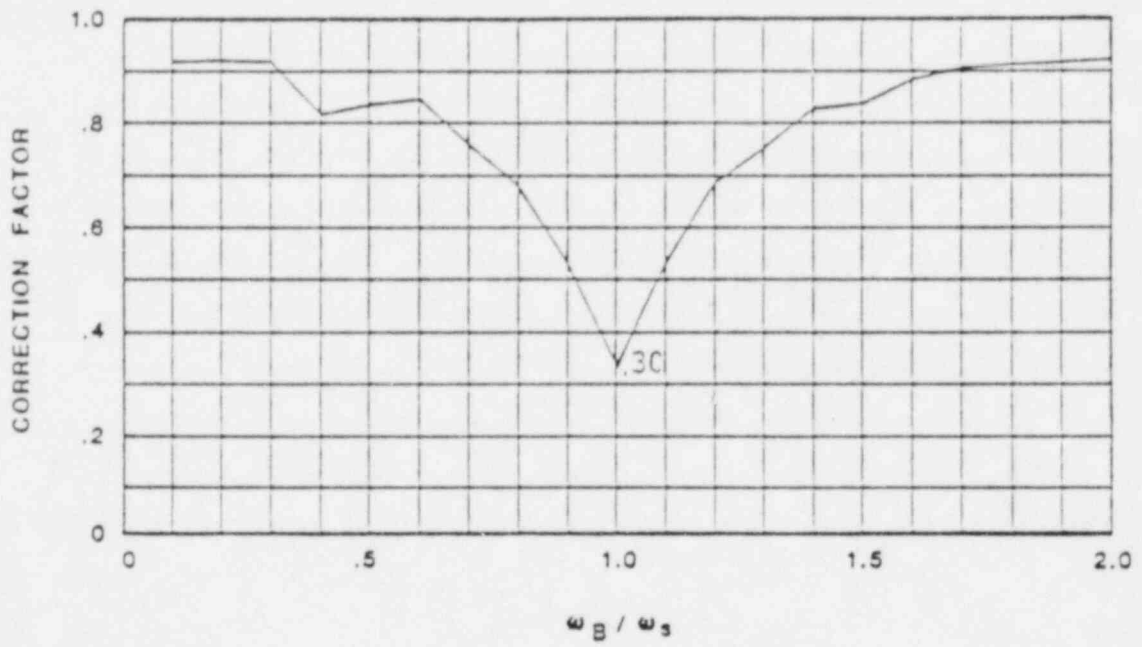


Figure 10.3-5 - Typical Modal Correction Factor

Question 10.3b

Provide justification for the applicability of these factors to "multidegree of freedom" systems since the factors were developed using simple "one degree of freedom" systems.

Response to Question 10.3b

The transient response of the Fermi 2 suppression chamber due to SRV torus shell loads is obtained using the modal superposition method. Using this approach, the equations of motion for a multi-degree of freedom system, such as the suppression chamber, are decoupled into a set of equivalent single degree of freedom systems. Each structural frequency or mode is represented by a single degree of freedom system. The responses of each single degree of freedom system are summed to obtain the total response of the suppression chamber.

During the summation process, modal correction factors obtained from PUAR Figure 2-2.4-5 are applied to the response of each single degree of freedom system for each suppression chamber frequency. As discussed in the response to question 10.3a, the modal correction factors are developed using single degree of freedom systems and are compatible for use in the modal superposition method since this method is completely linear.

Question 10.4

Provide justification for not considering the effect of bending moments in column analysis using interaction formulae.

Response to Question 10.4

Consideration of column bending moments using the interaction formula is necessary when compressive stresses or column buckling is a concern. Since the suppression chamber support columns for Fermi 2 are heavily reinforced and braced continuously along their length, as shown in Figure 2-2.1-7 of the PUAR, the effects of buckling are negligible. Furthermore, bending moments in the support columns are small since the columns are permitted to slide horizontally at their base. The support column loads shown in Table 2-2.5-4 are substantially below the allowable compressive loads for the support column wide flange sections with cover plates.

Question 10.5

With regard to the suppression chamber columns, provide justification and/or additional information to indicate why a nonlinear time history analysis was not performed as required by the criteria when net tensile forces are produced in the columns. Table 2-2.5-2 of PUA report indicates that net tensile forces are produced in the columns.

Response to Question 10.5

The criteria requirements for performing a non-linear time history analysis are applicable for plants in which the suppression chamber and its supports are not anchored to the basemat. Such a condition would result in gross non-linear behavior if uplift loads exceeded the weight of the suppression chamber and contained water.

The Fermi 2 suppression chamber is fully anchored to the basemat at each mitered joint column and saddle base plate location, as shown in PUAR Figures 2-2.1-7 and 2-2.1-8. Although tensile forces are produced in the column and saddle supports, the tensile forces are less than the allowable anchorage capacity of the support system, as shown in PUAR Table 2-2.5-4. The requirements for a non-linear analysis, therefore, need not be evaluated for Fermi 2 since the suppression chamber is fully anchored to the basemat and the effects of non-linearities on the overall suppression chamber response have been minimized.

Question 10.6

Provide justification for using two different temperatures, 173°F for suppression chamber and vertical support systems and 100°F for the base plate of the support system, for calculating the respective allowable stresses.

Response to Question 10.6

The allowable stresses for the suppression chamber and its vertical supports are conservatively determined at 173°F since this is the maximum temperature specified for any LOCA event, as shown in PUAR Figures 2-2.2-4 through 2-2.2-6. The allowable stresses for the vertical support system base plates are determined at 100°F which bounds the maximum temperatures of the base plate expected during the specified events. There may be long term conditions which result in higher base plate temperatures, however base plate temperatures higher than 100°F are not expected to occur during times of peak transfer of hydrodynamic loads to the suppression chamber vertical support system. Furthermore, the allowable stresses at 100°F and 173°F are not significantly different.

Question 11.1

Provide justification for using SRSS method to combine the SSE and LOCA responses for SRV piping analysis instead of the absolute sum or cumulative distribution function approaches as required by the criteria.

Response to Question 11.1

The method of combining responses due to LOCA and SSE loads for SRV piping described in Section 5-2.2.3 of the Plant Unique Analysis Report (PUAR) is based on NRC document NUREG-0484, Revision 1, "Methodology for Combining Dynamic Responses", published in May, 1980. The original issue of NUREG-0484 justified combination of responses due to LOCA and SSE within the reactor coolant pressure boundary using the SRSS technique. The current Revision 1 has extended the application of this combination technique to include ASME Section III, Class 1,2, and 3 systems, components and supports. As described in Revision 1, use of the SRSS technique provides a non-exceedance probability of 84 percent or higher. Since the Fermi 2 SRV piping is Class 2, the use of the SRSS method is acceptable based on Revision 1 of NUREG-0484.

Question 11.2

Provide justification for using Markl's equation for fatigue analysis of SRV piping instead of the SN curve given in ASME Code Section III, Division 1 Appendices.

Response to Question 11.2

The methodology for evaluating Fermi 2 SRV piping fatigue was originally presented to the NRC during a meeting in June of 1981 and was followed by a letter submitted to the NRC shortly thereafter (Reference 11.2-1). Section 3.9.3 of Supplement 1 of the Fermi 2 Safety Evaluation Report (NUREG-0798) references the required fatigue evaluation and the proposed methodology.

Since the SRV piping is a Class 2 system, the approach outlined in the presentation and letter was to evaluate fatigue using ASME Class 2 piping rules as a guideline. The proposed methods included extension of the Class 2 equations and curves used for thermal fatigue evaluation to include all cyclic loads. A comparison of the extended Class 2 method to a Class 1 fatigue analysis was also provided which showed that the two methods yield similar results.

Using the proposed methods, a fatigue usage factor is determined for each of the cyclic loadings. For Mark I LOCA related loads, estimates of total stress cycles during plant life would be determined and associated fatigue usage would be calculated. Since only very conservative estimates of the number of SRV

discharge related stress cycles were available, the approach proposed that SRV actuations would be monitored to assure that the allowable fatigue usage was not exceeded.

Following Detroit Edison Company's commitment to the NRC to perform an SRV piping fatigue evaluation, the matter was discussed between the NRC and the Mark I Owner's Group. These discussions resulted in a commitment by the Mark I utilities to perform fatigue evaluations for SRV piping in the torus and for torus attached piping systems as part of the plant unique analyses.

Discussions among Mark I Owners and their AE's followed and a task force was formed to develop a generic approach for fatigue evaluation. The approach agreed upon was a method which extended the Class 2 piping fatigue rules similar to the methods initially proposed for Fermi.

Refinements to the proposed Fermi 2 methods which have been incorporated into the generic approach consist of the following:

- o Fatigue usage is evaluated based on considering critical loading combinations instead of on an individual load basis.

- o Total cumulative fatigue usage for all cyclic loadings is calculated in lieu of monitoring SRV actuations.

- o The allowable number of stress cycles is determined by using Markl's equation (Reference 11.2-2) in lieu of the Class 2 thermal fatigue equation basis. (Markl's equation forms the basis for Class 2 piping fatigue and was used in developing the Class 2 piping Stress Intensification Factors).

- o Actual stress cycles for a given response time-history are converted into equivalent full stress cycles using the methodology defined in Section NC-3611.(e) (3) of the Code.

The SRV piping fatigue evaluation performed for Fermi-2 and documented in Volume 5 of the PUAR includes the extended Class 2 approach originally proposed for Fermi-2 and incorporates the additional refinements included in the generic Mark I approach. The refinements result in a more practical, comprehensive method of evaluation for fatigue.

Reference 11.2-1 - Detroit Edison Company Letter EF2-53,824 to NRC dated June 22, 1981.

Reference 11.2-2 - Markl, A.R.C., "Fatigue Test of Piping Components", Transactions ASME, Volume 74.

Question 11.3

Provide justification for not using Equation 11 of ASME Code Section III, Subsection NB for calculating the fatigue stresses, and explain the method used.

Response to Question 11.3

Justification for not using Equation 11 of ASME Code Section III, Subsection NB (Class 1 Piping) is provided in the response to Question 11.2. Equation 11 of Subsection NC (Class 2 Piping) of the ASME Code provides combination methods for thermal and other sustained loads used in evaluating for fatigue. The methods applied in the Fermi Plant Unique Analysis Report extended traditional usage of Equation 11 to combination of stresses due to dynamic cyclic loadings, using the same method of absolute summation of stresses.

Question 11.4

Provide justification and reference for the maximum-stress cycle factors given in Table 5-2.4-4 of the PUA report.

Response to Question 11.4

See the response to Question 11.2 for a description of the methodology for evaluating Fermi-2 SRV piping fatigue. The basis for developing R factors used to determine maximum equivalent full stress cycles is derived from the Class 2 piping thermal fatigue techniques defined in Section NC-3611.2(e)(3) of the Code. R factors for individual dynamic cyclic loadings also take into account consideration of loading characteristics such as frequency, time-history and random phasing of load components.

Question 11.5

Provide the magnitudes of the dynamic load factors used in Tables 5-3.2-1 to 5-3.2-3 of the PUA report and the justification.

Response to Question 11.5

The dynamic load factors (DLF) included in the loads specified in Tables 5-3.2-1 through 5-3.2-3 of the PUAR are summarized in the attached Table 11.5-1.

The loading functions for water jet impingement loads, T-quencher thrust loads, and T-quencher end cap thrust loads are defined as rectangular pulse loadings. The maximum DLF specified by standard structural dynamics handbooks for this type of load function is 2.0.

DLF's for SRV air bubble drag loads were determined using Monticello in-plant test data as permitted by NUREG-0661. The criteria states that actual measured pressure wave forms determined in tests may be used to develop a maximum structural amplification for resonant conditions. Using the measured Monticello pressure waveforms, a maximum DLF of 3.0 at resonant conditions was developed and is used for structures whose natural frequency is within the 4.0 to 14.0 Hz frequency range of the SRV air bubble drag loads. For structures whose natural frequency is well above the maximum air bubble drag load frequency a DLF of

2.0 is conservatively used. The natural frequencies of the T-quencher and its supports and the submerged SRV piping are sufficiently above the maximum air bubble drag load frequency, as shown in PUAR Figures 5-3.4-3 through 5-3.4-6.

Table 11.5-1

PUAR Dynamic Load Factors for SRV Piping, T-quencher,
and T-quencher Supports

Load Type	PUAR Table Number	Dynamic Load Factor (DLF)
SRV water jet impingement	5-3.2-1	2.0
SRV air-bubble drag	5-3.2-1 and 5-3.2-3	2.0
T-quencher and end cap thrust load	5-3.2-2	2.0

Question 11.6

Provide the results of the analysis of bolted or welded connections associated with the SRV piping.

Response to Question 11.6

The tables in the PUAR which contain analysis results for wetwell SRV piping major support connections and welds are shown in the attached Table 11.6-1. The referenced tables show that SRV piping wetwell support connection stresses are within allowable limits.

Table 11.6-1

PUAR Table References for Wetwell SRV Piping Support
Connections and Welds

Support Connection/Weld Stress	PUAR Table Number
Vent Line-SRV Piping Penetration and Welds	3-2.5-6
SRV Piping Vent Line and Vent Header Supports	5-2.5-5
Ramshead and T-quencher Arm Supports and Welds	5-3.5-4

Question 12.1

Provide justification for the method of lumping additional fluid masses along the ringbeam, quencher beam (Page 2-2.103 of PUA report), submerged length of SRV piping, T-Quencher and supports (Page 5-3.49 of PUA report) as indicated in the PUA report.

Response to Question 12.1

The hydrodynamic masses used for evaluating submerged structures are calculated using the relationships contained in PUAR Table 1-4.1-1 which are taken from LDR Table 4.3.4-1 (Reference 12.1-1). For the SRV piping, ramshead, T-quencher arms, 6 in. diameter lateral support members, and 20 in. diameter lateral support beam, the hydrodynamic mass equations for a circular cylinder were used. The hydrodynamic mass for the T-quencher arm ring plate supports are calculated using the equation for a circular disk. For the ring beam and vertical quencher support beam, the hydrodynamic mass is calculated using the equation for a plate in the lateral direction and an I-beam in the vertical direction.

Reference 12.1-1 - General Electric Report NEDO-21888, Revision 2, "Mark I Containment Program Load Definition Report", dated December, 1981.

Question 12.2

Provide justification for not considering the loads indicated in Table 1 which are required in the analysis according to NUREG-0661.

Response to Question 12.2

All loads specified by NUREG-0661 were addressed in the PUAR. The loads identified in Table 1 which are not included in Table 1-4.3-1 of the PUAR can be categorized as being negligible, not applicable to the Fermi plant, or are considered in the analysis. The loads circled in Table 1 are discussed in the paragraphs which follow.

4.3.5 Froth Impingement. The froth impingement loads on the torus shell are negligible as indicated in LDR Section 4-3.5-1. The torus support system will also have negligible effects due to the froth impingement. For SRV piping, the portion below the vent header is protected from pool swell impact loads by the vent header deflector. The portion below the vent line experiences negligible loads due to froth impingement.

4.3.8 LOCA Bubble Drag. The vent header support columns are the only structures above the bottom of the downcomers and below the normal water level. The LOCA bubble drag loads on these columns are contained in PUAR Table 3-2.2-9.

- 4.5.3 Chugging Vent System Loads. The chugging loads on the main vent and vent header were considered in the analysis and are contained in PUAR Table 3-2.2-19.
- 5.2.5 T-Quencher Air Bubble Drag. The SRV air bubble drag loads on these structures were considered in the PUAR. The SRV air bubble drag loads on the downcomers are given in PUAR Table 3-2.2-22. The SRV air bubble drag loads on the T-Quencher and the SRV piping are given in PUAR Table 5-3.2-3, and the SRV air bubble drag loads on the T-Quencher supports and vent header support columns are given in PUAR Tables 5-3.2-1 and 3-2.2-23, respectively.
- 5.2.6 Thrust loads on T-Quencher arms. The thrust loads on T-Quencher arms are given in PUAR Table 5-3.2-2.
- 5.2.7 SRVDL Environmental Temperatures. The SRV discharge line environmental temperature loads are discussed on page 5-3.17 of the PUAR.
- 5.3 Ramshead Loads. Ramshead loads are not applicable for Fermi 2 since the SRV Lines are equipped with the T-Quencher discharge devices rather than the ramsheads.

Question 12.3

Provide information on the analysis of the attachment welds of regions connecting the internal structures to the torus shell, indicating whether the criteria requirements have been satisfied.

Response to Question 12.3

The internal structure attachment welds to the torus shell have been evaluated in accordance with the criteria requirements. The attached Table 12.3-1 shows the most highly stressed catwalk and monorail support pad plate attachment welds to the torus shell. The load combinations for which the welds are evaluated are presented in PUAR Table 4-2.2-2. The welds are evaluated using the ASME Code criteria contained in Subsection NE for Class MC components. As can be seen from the attached table, the internal structure attachment weld stresses are within allowable limits.

Table 12.3-1

Catwalk and Monorail Support Pad Plate Weld Stresses

Item	Calculated Stress (ksi)	Allowable Stress (ksi)	<u>Calculated</u> <u>Allowable</u>
Catwalk Pad Plate Weld	3.46	15.01	0.23
Monorail Pad Plate Weld	0.49	15.01	0.03